A Dielectric, Mechanical, Rheological, and Electron Microscopy Study of Cure and Properties of a Thermoplastic-Modified Epoxy Resin

Alexander J. MacKinnon,† Stephen D. Jenkins,‡ Patrick T. McGrail,‡ and Richard A. Pethrick*,†

Thomas Graham Building, Department of Pure and Applied Chemistry, University of Strathclyde, 295 Cathedral Street, Glasgow G1 1XL, U.K., and ICI plc, Wilton Materials Research Centre, Wilton, Middlesbrough, Cleveland TS6 8JE, U.K.

Received November 8, 1991; Revised Manuscript Received February 15, 1992

ABSTRACT: Dielectric, mechanical, thermal, rheological, and electron microscopy measurements are reported on the effect of varying the proportion of a blended thermoplastic, poly(ether sulfone), on the cure and properties of an epoxy resin system, an aromatic diamine cured trifunctional aromatic epoxide. Data presented cover both changes in physical properties during cure and final properties of the cured matrix. The initial mixture, prepared by solution casting, is homogeneous, but phase separation occurs rapidly in the initial stages of curing. Dielectric, thermal, and rheological measurements obtained during the curing process are consistent with phase separation occurring within the resin. Analysis of the dielectric data obtained from fully cured materials demonstrates the existence of a relaxation process which can be ascribed to polarization of a conducting occluded phase. Correlation of these data with those obtained from electron micrographs indicates that the type of phase structure changes with thermoplastic content. A number of the mechanical properties are observed to change at about 20–25% (w/w) of incorporated thermoplastic, coincident with the occurrence of a cocontinuous phase. The effects of these changes in the morphology on the mechanical, dielectric, and thermal properties of this thermoplastic-modified thermoset are discussed.

Introduction

Thermoplastic modification of thermoset resin materials provides a solution to the problem of embrittlement observed in highly cross-linked thermosets[1-8] used in aerospace applications, where a tough continuous fiber composite is required. Thermoset-based systems are preferred due to their ease of processing—low temperature of cure, high tack, and drape, allowing complex shapes to be fabricated. Liquid carboxy-terminated butadiene–acrylonitrile copolymers (CTBN) are widely used with epoxy resins to generate rubber-toughened materials. During the curing process, the CTBN rubber phase separates into micron-sized domains; however, this has the disadvantage that the rubber particles reduce the T_g and modulus, and hence the resin performance in hot/wet conditions in comparison to the unmodified thermosets. Linear, high molecular weight thermoplastics are inherently tough and may be expected to reduce the brittleness of a thermoset without affecting their other properties significantly. Bucknall and Partridge[2] have used ICI's poly(ether sulfones) in epoxy resin to generate a high-temperature thermoplastic-modified thermoset. Subsequently, different thermoplastics have been studied in epoxy resins by Bucknall,[3] McGrath and co-workers,[4] and Sefton and co-workers.[5] Thermoplastics have also been studied in other types of thermoset networks.[6-8] The thermoplastics and thermosets used in this study were chosen to be thermodynamically compatible; however, during the curing process it is now recognized that the increasing molecular weight of the thermoset component initiates phase separation to generate a heterogeneous cured material.[9,10] Unlike CTBN, which tends to form a simple particulate morphology, the thermoplastic-modified epoxy resins may exist as homogeneous, particulate, cocontinuous, or phase-inverted morphologies.[5,8]

In the past few years, dielectric measurements have undergone a renaissance.[11-17] Application of microprocessor control to dielectric measurement has enabled real-time observation of the dipolar relaxation characteristics of thermosets undergoing cure. Increases in the viscosity associated with the curing process may be measured using conventional oscillatory cone-and-plate rheometers; however, it is rather difficult to use these instruments to monitor the change in viscosity over the whole process of cure.[18,19] An alternative approach to this problem has recently been published,[20] which allows the rheology to be monitored over the whole period of cure. In this paper, rheological and dielectric measurements are reported during cure, and thermal, dielectric, and mechanical characteristics are presented, together with electron micrographs of the completely cured thermoplastic-modified epoxy resin.

Experimental Section

Materials. The modified thermoset system was based on the cure of triglycidylaminophenol (Ciba Geigy MY0510) with 4,4′-diaminodiphenyl sulfone, (4,4′-DDS, Ciba Geigy HT976) and incorporating a thermoplastic, Victrex 5003P, poly(ether sulfone) (ICI plc). The epoxy resin and hardener were used as supplied in the ratio of 2.1:1 (w/w), while the thermoplastic was dried before use. Cure samples were made by first dissolving the thermoplastic in a 95:5 (% v/v) mixture of methylene chloride and methanol. The epoxy and hardener were then added before this solvent was mostly boiled off, leaving an apparently homogeneous solution. The blend was then poured into an open mold (dimensions 14 cm × 10 cm), which had been preheated to 140 °C, and degassed for 30 min under vacuum to remove residual solvent and trapped air. For dielectric and rheological measurements, the mold was removed from the oven, cooled rapidly to quench the curing reaction, and stored at −20 °C until used. The samples for mechanical testing were cured at 180 °C for a further 120 min and then allowed to cool to room temperature over a period of 120 min. A range of samples with varying thermoplastic content (0–40% (w/w)) was made in each case.

Dielectric Measurements. Measurements were performed using a Solartron 1250 frequency-response analyzer operating

* To whom correspondence should be addressed.
† University of Strathclyde.
‡ ICI plc, Wilton Materials Research Centre.

0024-9297/92/2225-3492$03.00/0

over a frequency range from 0.1 to 6 × 10^5 Hz. The frequency range was selected to allow collection of approximately 30 data points within a period of 3 min. Typically, the time taken for cure of the resin after reaching 180 °C was 100 min; hence the collection time is sufficiently short for the data to approximate to an instantaneous *snapshot* of the dielectric properties. A cell was designed which consisted of two pre-etched copper electrodes mounted on an epoxy glass fiber base separated by a copper spacer. This configuration generates a three-terminal electrode system with an active area of 1 cm^2. The space between the electrodes was maintained constant by soldering the copper spacer around three edges of the cell. Depending on the viscosity, either the initial mixture was heated and poured into the cell or, alternatively, a section was extracted from the frozen preplaque and inserted between the electrodes before soldering was carried out. The cell was attached to a heating block and placed in an Oxford Instruments cryostat (DN1704). The electrodes were in good thermal contact, and isothermal conditions were maintained using an Oxford Instruments ITC4 temperature controller. The method used for the dielectric measurements has been described elsewhere. Observations at predetermined times were stored automatically on file for subsequent analysis.

Rheological Measurements. A curometer, designed at Strathclyde, was used to monitor changes in the viscosity as a function of time and allow determination of the real and imaginary parts of the shear modulus at 2 Hz and also the curing exotherm occurring during cure.[20] The instrument was calibrated using Santovac-5, which was chosen because it exhibits a very high temperature–viscosity coefficient and forms a stable supercooled liquid state which has been studied extensively.[22,23]

Electron Microscopic Examination. Scanning electron micrographs were obtained using a Hitachi S-520 SEM. Samples obtained from the dielectric measurements were prepared for SEM examination by polishing with alumina and then etched with a 1% solution of potassium permanganate in a 5:2:2 volume mixture of concentrated sulfuric acid–phosphoric acid–distilled water. After etching, the samples were sequentially washed in aqueous sulfuric acid, hydrogen peroxide (100 volumes), water, and finally acetone. All samples were then sputter coated with gold before SEM examination.

Differential Scanning Calorimetry Measurements. Two series of DSC measurements were conducted in a Du Pont Model 9900 DSC. In all cases a sample of approximately 10 mg was used at a heating rate of 10 °C/min over a temperature range of −50 to +300 °C. In the first series of experiments the sample was cured during the first temperature scan to allow evaluation of the heat of reaction, then the sample was allowed to cool to room temperature over a period of 60 min, and a second scan was used to determine the final glass transition temperature. In a second series of experiments, measurements were carried out on samples from a series of plaques prepared for mechanical testing to estimate the degree of cure after 180 °C and also determine the final glass transition temperature of the material.

Mechanical Testing. The mechanical properties were assessed on molded plaques and the following derived: flexural strength, measured at 5 mm min^{-1} by a three-point bend test using a sample size of 50 mm × 10 mm × 3 mm; yield strength σ_y, measured in compression mode using a sample size of 10 mm × 10 mm × 3 mm; crack opening mode stress intensity factor K_{Ic}, measured at 1 mm min^{-1} using a sample size of 70 mm × 10 mm × 3 mm with a single edge notched on the 10-mm face; strain energy release rate for opening mode G_{Ic}, measured at 1 mm min^{-1} using a sample size of 70 mm × 10 mm × 3 mm with a single edge notch on the 10-mm face. All measurements were made at 23 °C. In addition, the ductility factor, $(K_{Ic}/\sigma_y)^2$, was derived from the measurements. The appropriate test methods have been reported elsewhere.[24]

Theory for the Analysis of Dielectric Behavior of Heterogeneous Systems

Previous studies of cured epoxy/thermoplastic blends have indicated that the final material forms a phase-separated structure and that the morphology depends critically on the level of thermoplastic in the matrix material. It is therefore of interest to be able to characterize further the point at which phase separation occurs and also its effects on a range of physical properties. Phase separation has been shown in thermoplastics to produce distinct dielectric behavior[24-30] which can be related to the polarization of mobile charges within conducting occlusions dispersed within the matrix. The observed dielectric dispersion associated with this polarization can be several orders of magnitude larger than that typically observed for dipolar relaxation. Studies on model systems and phase-separated polymers such as styrene–butadiene–styrene have shown that the dielectric process can be uniquely related to the morphological structure of these materials.

The dielectric properties of a polar organic material may be described in terms of the frequency dependence of the complex permittivity.

$$\epsilon^*(\omega) = \epsilon'(\omega) - i\epsilon''(\omega) \tag{1}$$

where $\epsilon'(\omega)$ and $\epsilon''(\omega)$ are the real and imaginary parts of the dielectric permittivity. In the case of a simple dipolar media, the frequency dependence of eq 1 has the form

$$\frac{\epsilon'(\omega) - \epsilon_\infty'}{\epsilon_0' - \epsilon_\infty'} = \frac{1}{1 + \omega^2\tau^2} \tag{2}$$

and

$$\frac{\epsilon''(\omega)}{\epsilon_0' - \epsilon_\infty'} = \frac{\omega\tau}{1 + \omega^2\tau^2} \tag{3}$$

where ϵ_0' and ϵ_∞' are respectively the low- and high-frequency limiting values of the dielectric permittivity for a process with characteristic relaxation time τ. Equations 2 and 3 are interrelated via a Laplace transform according to the Kramers–Kronig relationship.[31,32] Analysis of such data to produce information on the dipolar relaxation process has been presented elsewhere.[33,34]

Dielectric Properties of Heterophase Systems. Polarization occurs in heterogeneous dielectrics as a result of the accumulation of virtual charge at the interface between two media having differing permittivities and conductivities. The theory of heterogeneous dielectrics has been reviewed by van Beek.[26] In the case of spheres or ellipsoids of conductivity σ_2 and permittivity ϵ_2' dispersed in a homogeneous matrix (σ_1, ϵ_1') the dielectric properties are described by the Maxwell–Wagner–Sillars model (MWS); the characteristic relaxation time τ_{MWS} and low-frequency limiting value of the permittivity ϵ_0 are described as follows:

$$\tau_{MWS} = \frac{\epsilon_1' + A_a(1-v_2)(\epsilon_2'-\epsilon_1')}{\sigma_1 + A_a(1-v_2)(\sigma_2-\sigma_1)} \tag{4}$$

$$\epsilon_0 = \frac{\sigma_1[A_a(1-v_2) + v_2](\sigma_2-\sigma_1)}{\sigma_1 + A_a(1-v_2)(\sigma_2-\sigma_1)} + v_2\sigma_1\frac{\sigma_1 + A_a(\sigma_2-\sigma_1)(\epsilon_2'-\epsilon_1') - [\epsilon_1' + A_a(\epsilon_2'-\epsilon_1')](\sigma_2-\sigma_1)}{[\sigma_1 + A_a(1-v_2)(\sigma_2-\sigma_1)]^2} \tag{5}$$

and ϵ_∞ is the limiting value of the high-frequency permittivity

$$\epsilon_\infty = \frac{\epsilon_1' + [A_a(1-v_2) + v_2](\epsilon_2'-\epsilon_1')}{\epsilon_1' + A_a(1-v_2)(\epsilon_2'-\epsilon_1')}\epsilon_1' \tag{6}$$

where A_a is the depolarization factor along the applied field axis, v_2 is the volume fraction of the occluded phase, and ϵ_1' and ϵ_2' are the low-frequency limiting permittivities for phases 1 and 2. For the special case of spheres

Table I
Cure Data of MY0510/4,4'-DDS/5003P Blends at 180 °C

% (w/w) 5003P	vitrification time (min)			pot life (min)	gelation time (min)
	ϵ' [a]	ϵ'' [b]	σ_{dc} [c]	η_1 [d]	η_2 [e]
0.0	66.7	67.6	75.0	N/A	N/A
5.4	83.0	85.0	115.8	N/A	N/A
11.0	79.0	85.0	98.2	N/A	N/A
15.6	88.0	96.0	112.9	N/A	N/A
20.6	91.0	91.0	111.0	17.9	23.4
26.7	85.0	84.6	73.7	27.3	28.5
30.0	94.1	95.1	56.1	22.7	31.0
34.6	103.0	116.0	101.0	21.7	34.7
39.1	121.0	141.0	109.2	21.3	36.0

[a] Vitrification point from leveling off of ϵ' at 10^4 Hz. [b] Vitrification point from leveling off of ϵ'' at 10^4 Hz. [c] Vitrification point from leveling off of σ_{dc}. [d] Pot life from 5% increase in η. [e] Gel point from $\eta = 10^4$ Pa·s.

or ellipsoids of conductivity σ_2 and permittivity ϵ_2' dispersed in a homogeneous medium (ϵ_1', σ_1'), the depolarizing factor along the a-axis of the ellipsoid, A_a, has the following form:

For the case of prolate ellipsoids ($a > b$)

$$A_a = \frac{-1}{(a/b)^2 - 1} + \frac{a/b}{[(a/b)^2 - 1]^{1.5}} \ln \{(a/b) + [(a/b)^2 - 1]^{1/2}\} \quad (7)$$

where a is the length along the major axis and b is the length along the minor axis.

For the case of oblate ellipsoids ($a < b$)

$$A_a = \frac{1}{1 - (a/b)^2} - \frac{a/b}{[1 - (a/b)^2]^{1.5}} \arccos (a/b) \quad (8)$$

For the case of spheroids where $a = b$, $A_a = 1/3$.

In practical cases, for lossy material dispersed in a polymeric insulator, i.e, $\sigma_2 \gg \sigma_1$ and $v_2 \ll v_1$, the following relationships apply:

$$\tau_{MWS} \simeq \frac{\epsilon_1' + A_a(\epsilon_2' - \epsilon_1')}{A_a \sigma_2} \quad (9)$$

$$\epsilon_\infty \simeq \epsilon_1' \left[1 + v_2 \frac{\epsilon_2' - \epsilon_1'}{\epsilon_1' + A_a(\epsilon_2' - \epsilon_1')}\right] \quad (10)$$

The above equations provide the basis for analysis of the dielectric properties of heterogeneous materials and will be used to investigate the form of the dielectric response of the fully cured MY0510/4,4'-DDS/5003P samples.

Results and Discussion

The discussion of the cure will be divided into two parts: first, an examination of the changes which occurred during the cure process and, second, an examination of the properties of the fully cured material.

Curometer Data. The rheology of mixtures with varying thermoplastic content was examined using the Strathclyde curometer to determine the pot life and gel times.[20] The addition of thermoplastic to the thermoset matrix inhibits the cure as determined by the gel time, estimated as the point at which the viscosity reaches a value of 10^4 Pa·s (Table I). It was not possible to monitor the rheology of systems containing less than 20% thermoplastic at 180 °C due to the highly exothermic nature of the epoxy resin. At higher thermoplastic content the polymer acts as a diluent, inhibiting the reaction and reducing the rate at which heat is liberated.

Table II
DSC of Cure of MY0510/4,4'-DDS/5003P Blends

% (w/w) 5003P	ΔH_{cure} (J g^{-1}) [a]	T_g (°C) [b]	$\Delta H_{postcure}$ (J g^{-1}) [c]	T_g (°C) [d]
0.0	666.7	237.3	35.3	222.1
5.4	624.0	220.0	38.0	215.9
11.0	618.4	217.3	41.4	211.7
15.6	566.3	214.3	46.8	202.6
20.5	483.2	206.7	52.8	206.4
26.7	475.6	212.4	52.6	214.8
30.0	448.7	215.0	59.6	215.9
34.6	444.8	213.8	62.6	219.0
39.1	412.6	209.4	67.1	218.2

[a] Cure reaction. [b] Rerun of sample from (a); T_g determination. [c] Postcure reacton of samples prepared at 180 °C for mechanical testing. [d] Rerun of sample from (c); T_g determination.

DSC Measurements. The initial mixture and completely cured materials were subjected to DSC analysis. The initial trace for the epoxy resin was used to determine the magnitude of the curing exotherm, and the glass transition temperature was obtained from a second scan on the cured material. Variation of the heat of cure and the glass transition temperatures for the various compositions investigated are presented in Table II. The curing exotherm decreased linearly with increase in the thermoplastic content, and no significant deviations from simple additivity were observed. In this system, the glass transition temperature of the cured unmodified epoxy resin material differs significantly from the values of the epoxy/thermoplastic blends, thus indicating that the blends may have different properties from those of the original material. A single T_g was observed in all blends due to the close proximity of the T_g's of the individual components, and there is little variation of T_g with the amount of thermoplastic added to the epoxy/thermoplastic blends.

For the second series of experiments on the plaques prepared at 180 °C, all samples showed similar characteristics over the two consecutive temperature scans. After the first scan a peak was observed associated with completion of the cure reaction up to 300 °C. Comparison of these results with the total heat of the curing reaction gives an estimate of the degree of cure in these systems.

Electron Microscopic Examination. Electron micrographs were obtained for various blends (Figure 1). All the micrographs of materials containing thermoplastic exhibit phase-separated morphology. Below 20%, the occluded phase is thermoplastic-rich (Figure 1a); an increase in the thermoplastic content changes the occlusions from spherical to ribbon-like, and ultimately a cocontinuous phase is generated at a composition of approximately 20–25% (Figure 1b). At higher levels of thermoplastic, a phase-inverted structure is generated, with the occluded phase now being epoxy-rich (Figure 1c,d). In the case of the particulate phases, the size of the spherical structures is of the order of 0.4 μm, whereas in the phase-inverted region the occluded phase now has a size of 0.2 μm.

Mechanical Testing. The mechanical properties of the individual matrix components were measured (Table III) and illustrate the differences in strength and toughness of the epoxy and thermoplastic phases. An increase in the thermoplastic content in the blends leads to a progressive decrease in flexural modulus (Figure 2a). In the case of other modified epoxy resin systems, and in particular those incorporating CTBN, the inclusion of a rubber will lower the mechanical strength of the material.[3,36-38] The initial drop observed in T_g is not paralleled by the flexural modulus, indicating that phase separation is the most important factor determining the

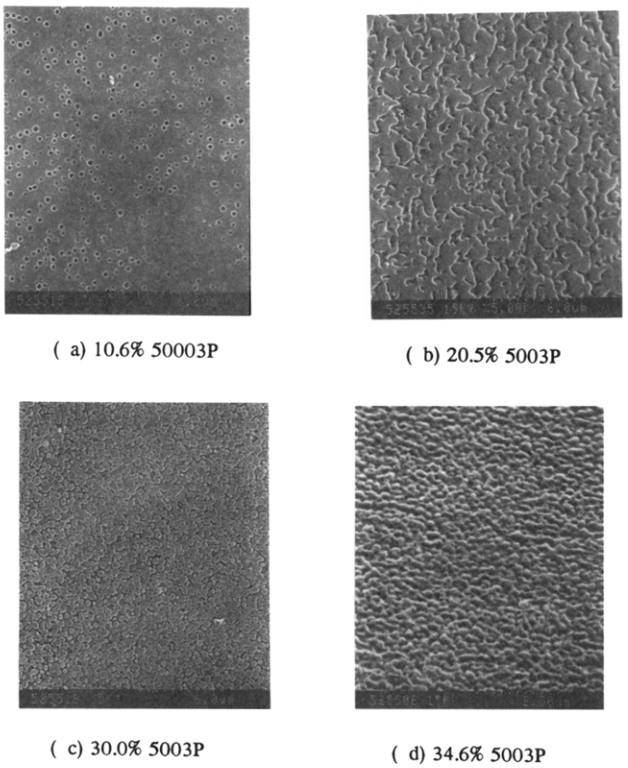

(a) 10.6% 50003P (b) 20.5% 5003P

(c) 30.0% 5003P (d) 34.6% 5003P

Figure 1. SEMs of cured specimens from dielectric studies: (a) 10.6% 5003P; (b) 20.5% 5003P; (c) 30.0% 5003P; (d) 34.6% 5003P, examined at non-normal incidence.

Table III
Mechanical Properties of Matrix Components[a]

material	E (GPa)	σ_y (MPa)	K_{Ic} (MN m$^{-3/2}$)	G_{Ic} (kJ m^{-2})
PES	3.2	78.0	2.6	2.0
cured MY0510/4,4′-DDS	3.71	202.5	0.66	0.15

[a] PES: E and σ_y measured at 23 °C and 1 mm min^{-1}; K_{Ic} and G_{Ic} measured at −65 °C and 1 m s^{-1} (PES data supplied by ICI). Epoxy: E and σ_y measured at 23 °C and 5 mm min^{-1}; K_{Ic} and G_{Ic} measured at 23 °C and 1 mm min^{-1}.

flexural modulus. The yield strength drops quite rapidly with increasing thermoplastic content (Figure 2b). Above 20% thermoplastic content, the leveling off of the yield strength is consistent with the continuous phase having become the thermoplastic. The fracture toughness (K_{Ic} and G_{Ic}) shows little variation with thermoplastic content up to the formation of a cocontinuous structure, but beyond this point there is a marked increase observed (Figure 2c,d). The efficiency of the thermoplastic as a toughener of the epoxy phase is rather poor; however, when it becomes the continuous phase, marked improvements in the properties are observed: K_{Ic} and G_{Ic} increase with a continuous decrease in the flexural modulus, and the yield strength and T_g reach a plateau and become composition insensitive.

Dielectric Measurements. Dielectric Analysis of the Cure Process. Measurements were performed on samples cured isothermally at 180 °C as a function of the composition of thermoplastic over the frequency range 10^{-1}–10^5 Hz. The three-dimensional plots for the 30% thermoplastic/epoxy blend are shown in Figure 3a, and all the traces showed three distinct relaxation features. At low frequency and short times, a large dielectric loss, which rapidly decreases as cure proceeds, is observed which is attributed to blocking electrode effects.[34,36] A high level of dc conductivity, characterized by an approximately ω^{-1} slope, is observed initially, and this is reduced during cure. However, in many of the samples a significant dc conductivity is still clearly evident in the fully cured matrix. The dipolar relaxation, observed as a peak in the loss at high frequencies and an increment in the dielectric constant, disappears after approximately 100 min and is associated with vitrification of the matrix.

The curves obtained with low levels of thermoplastic (5.4% (w/w)) are very similar to those obtained for the pure resin material. Further increase in the concentration of thermoplastic causes the dipolar process to become difficult to resolve. However, subtraction of the dc component from the observed relaxation allows identification of the dipolar process, and it is observed that vitrification is extended to longer times. The magnitude of the dc conductivity is reduced and an additional feature is observed in the finally cured material for compositions greater than 20% of thermoplastic (Figure 3). At a composition of 26.7% of thermoplastic and above, this feature has now developed into a distinct relaxation process independent of the time of cure.

The curing process leads to a reduction in the dc conductivity as a function of time (Figure 4). The initial high conductivity of the mixture progressively decreases in time, approaching an asymptotic level at long times. It has been pointed out previously[41] that the generation of a three-dimensional matrix would significantly inhibit the mobility of charge carriers through the matrix and hence is an indication of the gelation point. However, if the conduction process is dominated by the segmental mobility, then this point is indicative of vitrification. The vitrification point obtained from the intercept of the initial and final conductivity curves is listed in Table I and increases progressively with the addition of thermoplastic material, showing that the addition of the thermoplastic inhibits cure. Vitrification, the point at which dipolar reorientation ceases, can be determined by plotting the dielectric constant and loss as a function of time at a frequency of 10 kHz. The point at which the dielectric constant and loss reach an asymptotic value can be used as an indication of vitrification, and the results of this analysis are presented in Table I. The level of the residual dc conductivity varies with the thermoplastic content (Figure 5). A marked drop is observed at approximately 20% of incorporated thermoplastic. Table IV illustrates the electrical properties of the individual matrix components and clearly shows that the epoxy component is the more conducting phase.

The data on vitrification obtained from analysis of the variation with tie of ϵ' and ϵ'' are in good agreement with one another and illustrate the inhibition effect of the thermoplastic on cure. The ϵ'' data are obtained after subtraction of the dc component, and this confirms the validity of the procedure used.

The dielectric loss peak observed in the final cured matrix is associated with the phase-separated structure of the matrix, and careful analysis of the data indicates that the phase-separated structure is generated within the first two observations ca. within 6 min and is consistent with visual and related scattering studies on this system.[9,10]

Dielectric Analysis of the Fully Cured Material. The dielectric spectrum of the cured material contains two features: first, a contribution to the loss associated with dc conductivity and, second, a loss process only observed in the higher thermoplastic content materials. This latter process is attributed to the MWS effect. An SEM examination of the materials produced in this study indicates a systematic variation of the morphology with thermoplastic content (Figure 1a–d). At low thermoplastic

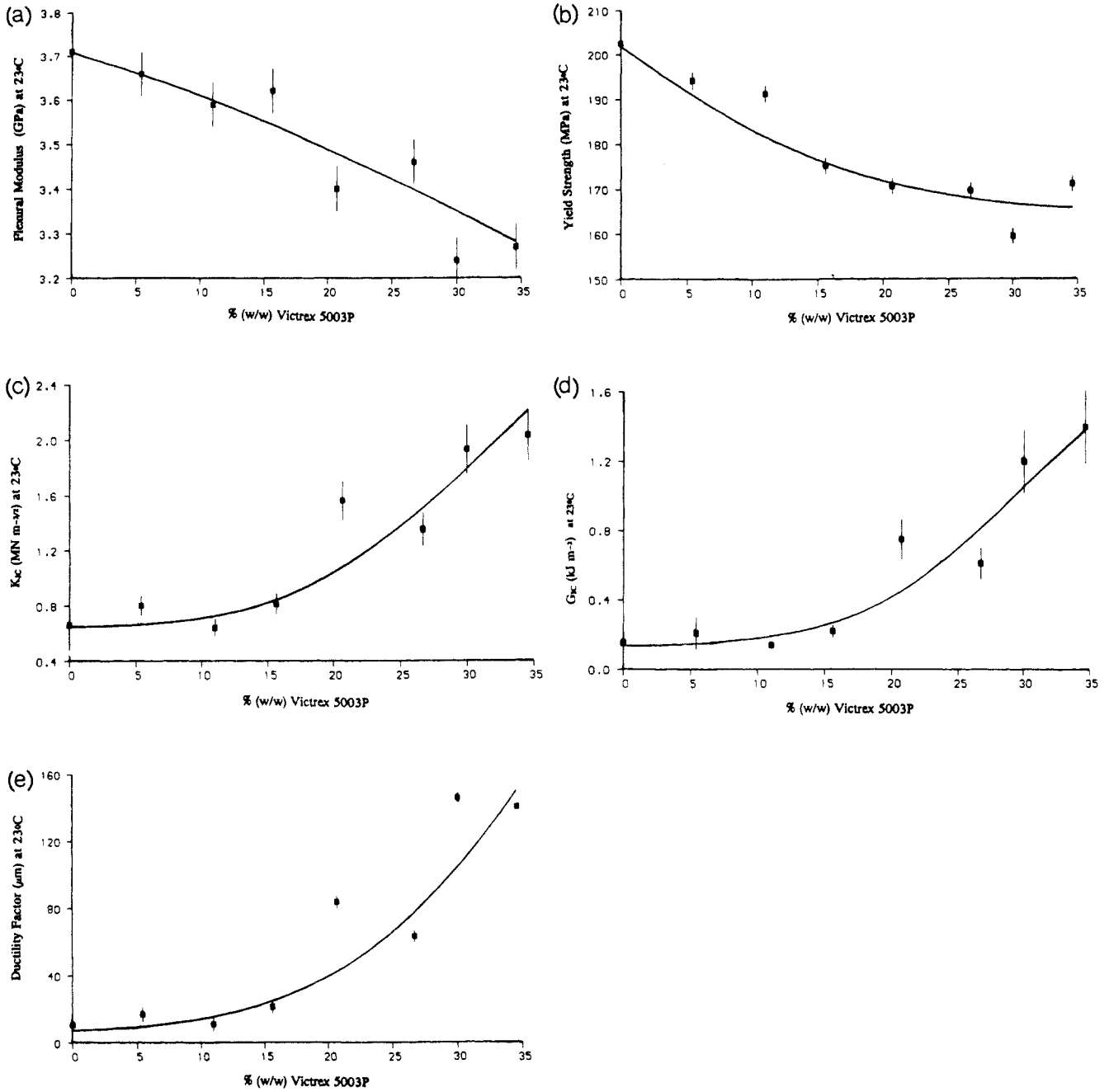

Figure 2. (a) Flexural modulus of MY0510/4,4′-DDS/5003P cured at 180 °C. (b) Yield strength of MY0510/4,4′-DDS/5003P cured at 180 °C. (c) K_{Ic} values for MY0510/4,4′-DDS/5003P cured at 180 °C. (d) G_{Ic} values for MY0510/4,4′-DDS/5003P cured at 180 °C. (e) Ductility factor of MY0510/4,4′-DDS/5003P cured at 180 °C.

contents, a particulate morphology is observed, the occluded phase being thermoplastic-rich. Correlation of the morphology obtained from the SEM study with variation in the dielectric properties indicates that the MWS feature can be associated with the occurrence of the phase-inverted morphology in the material. This is consistent with the MWS model, which requires the occluded phase to have a higher conductivity than the surrounding matrix and for a significant magnitude to be observed should approximate to an oblate spheroid.

To separate the MWS feature from the conductivity, it is necessary to subtract from the loss a contribution which varies according to $1/\omega$. Figure 6 illustrates the application of the subtraction process; the resultant dielectric loss curve is significantly broader than would be predicted by the simple Debye process, indicating a distribution of relaxation processes. This observation is consistent with the possible distribution in the morphological structure of the material. Detailed analysis of the position and amplitude of this process indicates that it varies significantly with composition of thermoplastic, reflected in the changes in the MWS fitting parameters (Table V). The MWS feature was observed once the thermoplastic levels were greater than 20.6%.

The main parameters in the MWS theory are the volume fraction, V_f, and conductivity, σ, of the occluded conducting phase, the dielectric constant of the matrix, ϵ_∞, and the shape of the occluded phase, defined in terms of the length a to breadth b projected in the field direction. The dielectric constant of the matrix is, however, not a variable as it is determined experimentally from the frequency plots. The shape of the loss curve is very sensitive to the subtraction of the dc conductivity; too large a value artificially sharpens the peak by reducing the amplitude at low frequency whereas too small a value leads to the reverse effect. To carry out this analysis, it is essential that the dielectric constant and loss are measured to low frequency, ca. 10^{-1} Hz. The conductivity of the occluded

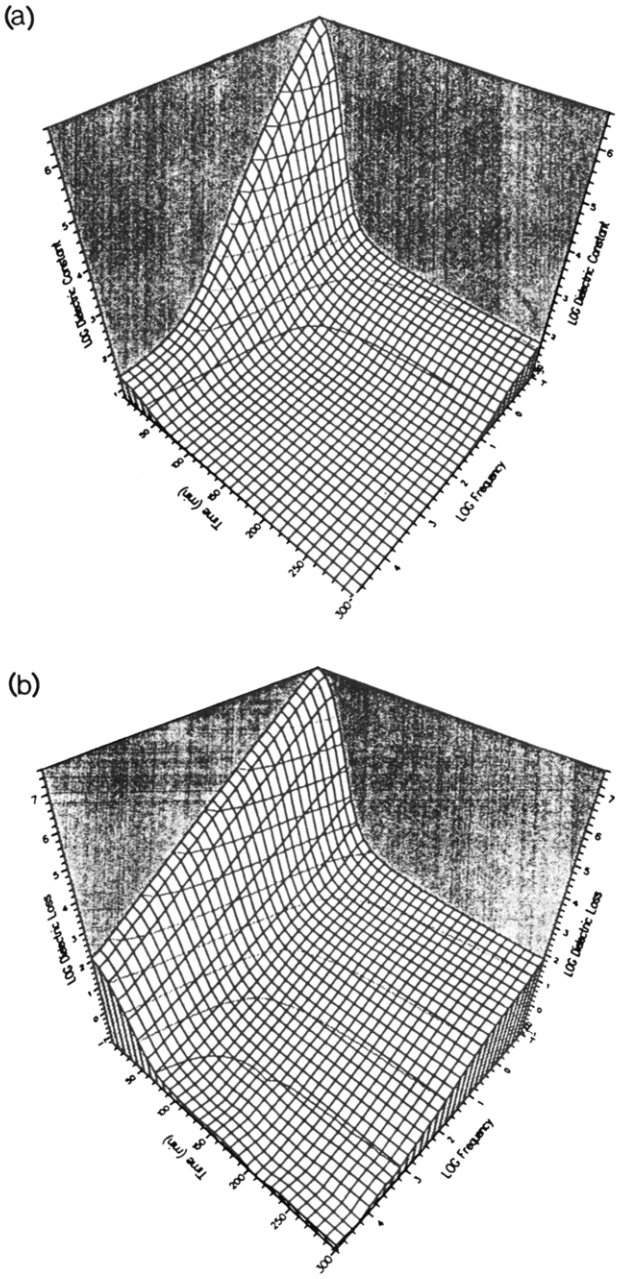

Figure 3. Cure of MY0510/4,4′-DDS/30.0% 5003P at 180 °C: (a) dielectric constant measured as a function of frequency/time; (b) dielectric loss measured as a function of frequency/time.

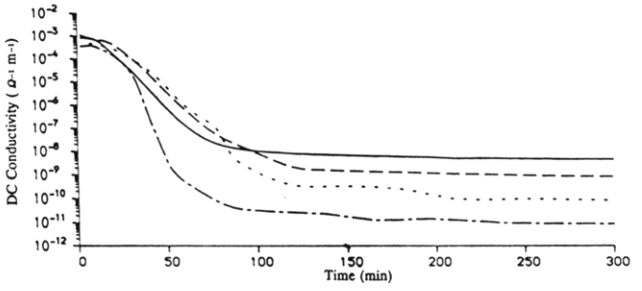

Figure 4. Dc conductivity monitored during the cure of MY0510/4,4′-DDS/5003P blends at 180 °C: (—) 0.0% 5003P; (– – –) 11.0% 5003P; (- - -) 20.5% 5003P; (– - –) 30.0% 5003P.

phase is determined by adjusting the theoretical prediction to give a good fit of the high-frequency side of the MWS peak. This subtraction procedure is very sensitive to the value chosen and allows the value of the dc conductivity to be accurately determined.

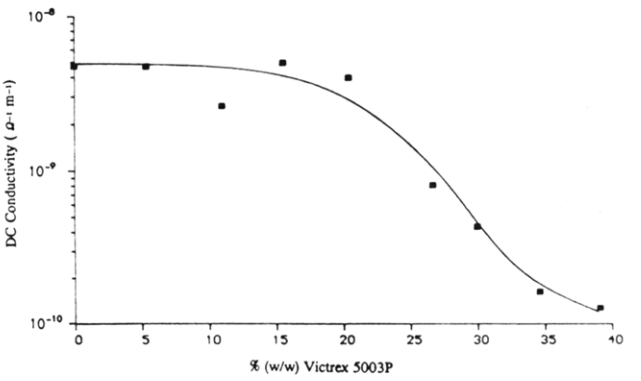

Figure 5. Residual dc conductivity of cured MY0510/4,4′-DDS/5003P blends measured at 180 °C.

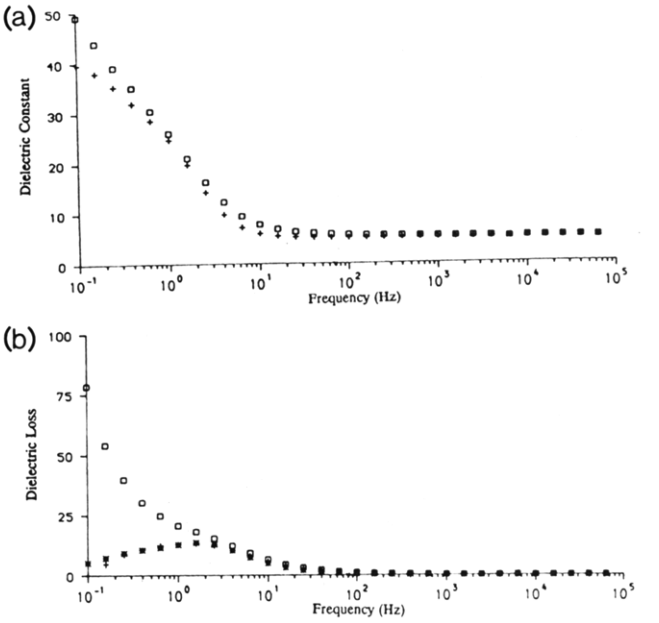

Figure 6. (a) Experimental and theoretical plots of dielectric constant of cured MY0510/4,4′-DDS/30.0% 5003P measured at 180 °C: (□) dielectric constant (experimental); (+) dielectric constant (theoretical). (b) Experimental and theoretical plots of dielectric loss of cured MY0510/4,4′-DDS/30.0% 5003P measured at 180 °C: (□) dielectric loss (experimental); (+) dielectric loss – dc conductivity (experimental); (*) dielectric loss (theoretical).

Table IV
Electrical Properties of Matrix Components at 180 °C

component	ϵ'	σ_{dc} (Ω^{-1} m^{-1})
Victrex 5003P	3.3	0.212×10^{-11}
cured MY0510/4,4′-DDS	8.9	0.483×10^{-8}

Initially the fitting was attempted using a morphology consisting of a single component and comparison was made with the experimental data. The volume fraction was obtained from chemical analysis and is not an adjustable parameter; the a/b ratio was the only adjustable variable in fitting the data. The prediction of theory showed poor agreement with experiment, and the calculation was refined to allow the occluded phase to be described in terms of a two-component distribution. This procedure will alter the shape of the relaxation process but will not move it on the frequency axis. In practice, it was found that a small adjustment of the conductivity value was also necessary to obtain agreement between experiment and theory for the high-frequency side of the loss. The values of the conductivity obtained were in general lower than those for the pure conducting phase. If a small amount

Table V
MWS Fitting Parameters for Cured MY0510/4,4'-DDS/5003P at 180 °C

% (w/w) 5003P	ϵ'	σ (Ω^{-1} m^{-1})	V_f	a/b
20.5	7.8	5.0×10^{-10}	0.80	0.07
			0.02	5.00
26.7	5.3	1.5×10^{-9}	0.70	3.25
			0.04	10.00
30.0	5.1	1.0×10^{-9}	0.65	2.40
			0.05	10.00
34.6	4.2	4.7×10^{-10}	0.60	1.90
			0.05	7.5
39.1	3.8	4.0×10^{-10}	0.55	1.49
			0.05	6.9

of the less conducting PES is dissolved in the epoxy matrix, it will lead to a reduction in the conductivity, consistent with the trends observed (Table V). This is also in agreement with previous studies of the thermodynamics of mixing of related systems.[9,10] Having fixed the conductivity, the total volume fraction defined by chemical analysis was then adjusted between the two morphologies to give a better fit of the dielectric loss.

In practice, the fit of the data is quite sensitive to the a/b ratio. In every case there is a significant low-frequency contribution to the dielectric constant, and this is modeled by the addition of the second component of high a/b ratio. Morphologically this is consistent with the occurrence of a very small amount of the cocontinuous–high aspect ratio matrix in the occluded phase. The most apparent feature from the MWS analysis is the variation of the shape factor, a/b, upon the level of thermoplastic. For this particular range of materials, with the exception of the blend with 20.5% 5003P, the a/b ratio associated with larger volume fraction decreases with increasing thermoplastic level. This is consistent with the observed changes in the shape of the occluded phase as determined by electron microscopy (Figure 1) and illustrates the tendency of the occluded phase to approach a more spherical form as the thermoplastic content is increased.

The occurrence of the MWS feature in a variety of thermoplastic and thermoset materials has been reported previously,[25-32,42,43] however, this is the first attempt to use the theory to gain a description of the shape and volume fraction distribution of the conducting occluded phases for a thermoplastic-modified thermoset system. The earlier studies[42,43] identified correctly the origins of the process; however, the imprecision of the data available made detailed comparison between theory and experiment difficult. The only adjustable variables in the theory related to the description of the morphology and indicate the potential of dielectric measurements for morphological characterization. It is only recently that the availability of computer-assisted dielectric measurements over an extended frequency range has made possible the accurate determination of the shape of the MWS curves. Dielectric measurements are made on bulk samples and hence the information obtained on the morphological distribution is not subject to the problems of interpretation associated with electron microscopy. Sectioned cylinders and ribbons can in electron micrographs appear as spheres and lead to misinterpretation of the structure of the material; this is not a problem with dielectric measurements since these structures have distinctly different values of the a/b ratio.

General Conclusions

In this paper the effect of variation of the thermoplastic content on the properties of an epoxy/thermoplastic blended matrix, which is initially homogeneous and then undergoes rapid phase separation on curing, is examined and shown to have a pronounced effect on the mechanical properties of these materials. The use of real-time dielectric measurements for in-situ monitoring of the cure of a phase-separating system is illustrated in this paper for the first time, and also its application to the characterization of the morphological distribution has been discussed. Hitherto, the dielectric technique has predominantly been used for dipolar relaxation characterization, and this paper illustrates the potential of the method as a tool for morphological characterization of phase-separated structures. Subsequent publications will consider the effect of changes in epoxy matrix composition, and the molecular weight and functionality of the thermoplastic on the phase separation and properties of these materials.

Acknowledgment. We thank the SERC and ICI plc for financial support (A.J.M.) and ICI plc for the provision of equipment, materials, test facilities, and overall support. Thanks are also due to Dr. D. Hayward, University of Strathclyde, for technical assistance throughout this work.

References and Notes

(1) Bucknall, C. B.; Partridge, I. K. *Polym. Eng. Sci.* **1986**, *26*, 54.
(2) Bucknall, C. B.; Partridge, I. K. *Polymer* **1983**, *24*, 639.
(3) Bucknall, C. B.; Gilbert, A. H. *Polymer* **1989**, *30*, 213.
(4) Cecere, J. A.; Senger, J. S.; McGrath, J. M. *32nd Int. SAMPE Symp.* **1987**, 1276.
(5) Sefton, M. S.; McGrail, P. T.; Peacock, J. A.; Wilkinson, S. P.; Crick, R. A.; Davies, M.; Almen, G. *19th Int. SAMPE Tech. Conf.* **1987**, 700.
(6) Shimp, D. A.; Hudock, F. A.; Bobo, W. S. *18th Int. SAMPE Tech. Conf.* **1986**, 851.
(7) Stenzenberger, H. D.; Romer, W.; Herzag, M.; Konig, P. *33rd Int. SAMPE Symp.* **1988**, 1546.
(8) Sefton, M. S.; McGrail, P. T.; Eustace, P.; Chisholm, M.; Carter, J. T.; Almen, G.; MacKenzie, P. D.; Choate, M. *3rd Int. Conf. Crosslinked Polym.* **1989**.
(9) Yamanaka, K.; Inoue, T. *Polymer* **1989**, *30*, 662.
(10) Ohnaga, T.; Maruta, J.; Inoue, T. *Polymer* **1989**, *30*, 1845.
(11) Senturia, S. D.; Sheppard, N. F. Dielectric Analysis of Thermoset Cure. In *Epoxy Resins and Composites IV*; Dusek, K., Ed.; *Adv. Polym. Sci.* **1986**, *80*, 1.
(12) Bidstrup, W. W.; Sheppard, N. F.; Senturia, S. D. *Polym. Sci. Eng.* **1986**, *26*, 358.
(13) Bromberg, M. L.; Day, D. R.; Snable, K. R. *Elec. Insul.* **1986**, *2*, 18.
(14) Sanjana, Z. N. *Polym. Sci. Eng.* **1986**, *26*, 358.
(15) Zukas, W. X.; Schneider, N. S.; MacKnight, W. J. *Polym. Prepr. (Am. Chem. Soc., Div. Polym. Chem.)* **1984**, *25*, 205.
(16) Sanjana, Z. N.; Selby, R. L. *Proc. 29th SAMPLE Symp.* **1984**, 1233.
(17) Bidstrup, W. W.; Senturia, S. D. *Polym. Eng. Sci.* **1989**, *29*, 290.
(18) May, C. *Chemorheology of Thermosetting Polymers*; *ACS Symp. Ser. No. 227*; American Chemical Society: Washington, DC, 1983.
(19) Dawkins, J. *Developments in Polymer Characterization*; Applied Science Publishers: Englewood Cliffs, NJ, 1982.
(20) Hayward, D.; Trottier, E.; Collins, A.; Affrossman, S.; Pethrick, R. A. *J. Oil Colour Chem. Assoc.* **1989**, Issue 11, 452.
(21) Hayward, D.; Mahboubian-Jones, M. G. B.; Pethrick, R. A. *J. Phys. E* **1984**, *17*, 683.
(22) Barlow, A. J.; Erginsav, A.; Lamb, J. *Proc. R. Soc. London, A* **1969**, *A309*, 473.
(23) Cochrane, J.; Harrison, G. *J. Phys. E* **1972**, *5*, 47.
(24) Davies, M.; Moore, D. R. *Compos. Sci. Technol.* **1991**, *40*, 131.
(25) Meakins, R. J. *Prog. Dielectr.* **1961**, *3*, 151.
(26) Van Beek, L. K. H. *Prog. Dielectr.* **1967**, 7, 69.
(27) Hanai, T. In *Emulsion Science*; Sherman, P., Ed.; Academic Press: London, 1968.
(28) Baird, M. E. *Electrical Properties of Polymeric Materials*; Plastics and Rubber Institute: London, 1973.
(29) Hedvig, P. *Dielectric Spectroscopy of Polymers*; Adam Hilger: Bristol, 1977.
(30) North, A. M.; Pethrick, R. A.; Wilson, A. D. *Polymer* **1978**, *19*, 913.
(31) North, A. M.; Pethrick, R. A.; Wilson, A. D. *Polymer* **1978**, *19*, 923.

(32) Siriwittayakorn, T. Ph.D. Thesis, University of Strathclyde, 1991.
(33) McCrum, N.; Read, B.; Williams, G. *Anelastic and Dielectric Effects in Polymer Solids*; John Wiley and Sons: New York, 1967.
(34) Hill, N. E.; Vaughan, W. E.; Price, A. H.; Davis, M. *Dielectric Properties and Molecular Behaviour*; Van Nostrand Reinhold Co.: New York, Toronto, and Melbourne, 1969.
(35) Daly, J. H.; Guest, M. J.; Hayward, D.; Pethrick, R. A. *Polym. Commun.* **1990**, *31*, 325.
(36) Daly, J. H.; Pethrick, R. A.; Fuller, P.; Cunliffe, A. V. *Polymer* **1981**, *22*, 33.
(37) Kinloch, A. J.; Shaw, S. J.; Tod, D. A.; Hunston, D. L. *Polymer* **1983**, *24*, 1341.
(38) Kinloch, A. J.; Shaw, S. J.; Hunston, D. L. *Polymer* **1983**, *24*, 1355.
(39) MacDonald, J. R. *Phys. Rev.* **1953**, *92* (1).
(40) MacDonald, J. R. *J. Electrochem. Soc.* **1988**, *135*, 2274.
(41) Lairez, D.; Emery, J. R.; Durrand, D.; Hayward, D.; Pethrick, R. A. "Real Time Dielectric Measurements of Network Formation in a Crosslinked Epoxy Resin System", to be published in *Plast. Rubber Process. Appl.*
(42) North, A. M.; Reid, J. C. *Eur. Polym. J.* **1972**, *8*, 1129–1138.
(43) Vallance, M. A.; Yeung, A. S.; Cooper, S. L. *Colloid Polym. Sci.* **1983**, *261*, 541–554.

Registry No. (MY0510)(HT976) (copolymer), 111481-61-9; Victrex 5003P, 25667-42-9.